*fluids*

MDPI

*Article*

# The Method of Image Singularities Employed for Oscillating Oblate Spheroids under a Free Surface

**Eirini I. Anastasiou [1], Eva Loukogeorgaki [2,*] and Ioannis K. Chatjigeorgiou [1]**

[1] School of Naval Architecture and Marine Engineering, National Technical University of Athens, 15780 Athens, Greece; eiranasta@gmail.com (E.I.A.); chatzi@naval.ntua.gr (I.K.C.)

[2] Civil Engineering Department, Aristotle University of Thessaloniki, 54124 Thessaloniki, Greece

* Correspondence: eloukog@civil.auth.gr; Tel.: +30-2310-99-5951

Received: 31 March 2020; Accepted: 15 May 2020; Published: 17 May 2020


**Abstract:** The main objective of this study is to develop a semi-analytical formulation for the radiation problem of a fully immersed spheroid in a liquid field of infinite depth. The term "spheroid" refers herein to the oblate geometry of arbitrary eccentricity and to the axisymmetric case, where the axis of symmetry is normal to the free surface. The proposed numerical approach is based on the method of image singularities, and it enables the accurate and fast calculation of the hydrodynamic coefficients for the translational degrees of freedom of the oblate spheroid. The excellent agreement of the results, with those of other investigators for the limiting case of the sphere and with those obtained using a respected boundary integral equation code, demonstrates the accuracy of the proposed methodology. Finally, extensive calculations are presented, illustrating the direct impact of the immersion depth and the slenderness of the spheroid on the hydrodynamic coefficients.

**Keywords:** image singularities; Miloh's theorem; hydrodynamics; radiation; oblate spheroids

## 1. Introduction

The interaction of surface waves with submerged spheres and spheroids presents a characteristic problem in the field of hydrodynamics. Considering the case of perfectly symmetric spherical geometries, Linton [1], for example, studied the diffraction and the radiation problem of a submerged sphere in waters of finite depth, while Wu et al. [2] extended Linton's work by including the calculation of drift forces. Rahman [3] studied the exciting forces of a submerged sphere, and estimated the wave elevation above the sphere due to monochromatic incident waves. All these studies employed Thorn's [4] multipole expansions, in order to expand the potential into series of spherical harmonics. On the other hand, in the case of spheroidal geometries, most existing studies focus on prolate spheroids, while relevant analytical solutions have been developed by utilizing the so-called system of image singularities. Briefly, the system of image singularities of an arbitrary exterior potential field within a spheroid allows the expression of the fundamental solution of the Laplace equation, i.e., the sources, in terms of spheroidal harmonics. Accordingly, it enables the implementation of a full hydrodynamic analysis based explicitly on the associated coordinate system. The analysis sought is performed by constructing the involved velocity potentials in terms of spheroidal harmonics.

The theorem on the system of image singularities for a spheroidal geometry, and the associated homonymous method, were first developed, and employed, by Havelock [5], who studied the moment, due to surface waves, applied on a fully submerged, moving prolate spheroid. Havelock [6] used the same method to investigate both the forces and the moments acting on a submerged moving prolate spheroid as the body is subjected to regular waves. In both cases, he studied, without a proof of the relevant theorem, the non-axisymmetric case, where the axis of symmetry of the spheroid is parallel to the undisturbed free surface. The proof of the theorem for a prolate spheroid was later

given by Miloh [7]. Subsequently, this theorem was employed by Chatjigeorgiou and Miloh [8–12], who investigated the diffraction, radiation and the wave resistance problems, for immersed prolate spheroids and for the non-axisymmetric case (symmetrical axis parallel to the undisturbed free surface). It should be noted that the works of Chatjigeorgiou and Miloh [8–12] preceded the studies of Wu and Eatock Taylor [13,14], who based their research on a Fredholm integral equation of the second type, involving a source/sink distribution over the surface of the spheroid. In terms of the "symmetric" placement of a prolate spheroid relative to the free surface, i.e., symmetrical axis normal to the free surface, it appears that the only relevant study is that of Chatjigeorgiou [15], who, however, started from Thorn's [4] multipoles in spherical coordinates, and developed rigorous addition theorems to transform the governing expansions into prolate spheroidal coordinates.

The relevant theorems, associated with the system of image singularities for an oblate geometry, were first reported in the book of Chatjigeorgiou [16]. Chatjigeorgiou et al. [17] utilized for the first time the method of image singularities in oblate geometry, to enable the solution of the diffraction problem for an immersed oblate spheroid in infinite water depth. The axisymmetric placement of the spheroid (symmetrical axis normal to the free surface) was considered. Indeed, the diffraction problem provides the path for the solution of the radiation problem, the case that is considered herein. The present investigation is a follow-up of the study conducted in [17], which, contrary to [17], determines and discusses the variation of the most important hydrodynamic parameters of added masses and hydrodynamic damping. The same formulation can be effectively extended to finite water depth as well.

A question which easily arises is whether the formulation(s) developed and analyzed herein can be immediately extended to prolate geometries with symmetrical placement relative to the undisturbed free surface. The answer cannot be strict and unconditional, given the different starting points of the existing (and reported) "image singularity systems" in prolate and oblate geometries. The former (e.g., [7]) rely on the uniform distribution of singularities along the major axis of the spheroid between the two foci, while the latter rely on the distribution of singularities on the fundamental disk of the oblate spheroid (e.g., [16]). The formulations are not by default equivalent, while the verification that they could coincide with only simple transformations would require some further mathematical elaborations.

The present paper focuses on the semi-analytical formulation of the radiation problem, for a fully submerged axisymmetric oblate spheroid in a liquid field of infinite water depth. The study employs the theorem of image singularities connected with the concerned geometry. The body is assumed to undergo small amplitude oscillations in all three translational modes of motion, while the rotational modes are considered ideally restricted. The solution of the problem relies on the use of the governing Green's function, and its transformation into oblate spheroidal coordinates via the evaluation of the Green's function multipoles. The velocity potentials for the radiation problem are expressed in a series of multipoles, which are appropriately truncated; thus, a semi-analytical formulation of the examined problem is realized. Simple formulas are, finally, derived, enabling the calculation of the hydrodynamic coefficients for the translational modes of motion. For demonstrating the reliability, the accuracy, and the robustness of the developed method, results are, initially, compared with those of Wu [18] for the limiting case of a sphere, and with those obtained using the respected Boundary Integral Equation (BIEM) code WAMIT [19]. Results are also presented focusing on the effect of the immersion depth and the slenderness of the spheroid on the hydrodynamic coefficients. Although the proposed method requires several mathematical processes/computations, its value is significant since it provides results in practically 'no time', and thus, it is characterized by computational efficiency. Moreover, the proposed numerical formulation can be extended for calculating the hydrodynamic coefficients of a semi-immersed oblate or arrays of oblates (fully submerged or semi-immersed). This is very important, as the oblate spheroid represents a promising configuration/shape for wave energy converters [20].

This study is organized as follows: In Section 2, the oblate spheroidal coordinate system, utilized throughout this work, is presented. Section 3 describes the examined boundary value problem, while in Section 4 we derive the formulas of the radiation velocity potentials. Section 5 includes the expressions of the added mass and the radiation damping coefficients. In Section 6 the results of this paper are presented and discussed in detail, while, finally, in Section 7 the main conclusions of the present investigation are cited along with suggestions for future work.

## 2. The Oblate Spheroidal Coordinate System

We study the axisymmetric configuration of the spheroid. The term "axisymmetric" refers to the case where the symmetrical axis of the spheroid is normal to the free surface. The center of the spheroid is assumed to be immersed at a distance $f$ below the undisturbed free surface. A Cartesian (global) coordinate system $(x, y, z)$ is assumed fixed on the undisturbed free surface, with its vertical $z$ axis pointing in the gravity direction. The origin of the local Cartesian system $(x, y, z^*)$ is taken fixed at the center of the body, with the vertical $z^*$ axis pointing, again, downwards, so that $z = z^* + f$ (Figure 1).

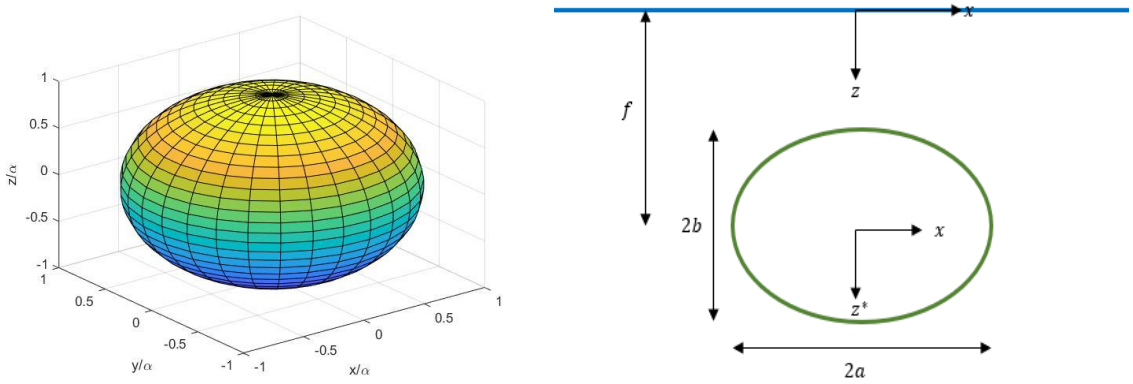


(**a**) (**b**)

**Figure 1.** (**a**) A 3D image of an axisymmetric oblate spheroid; (**b**) A 2D schematic of the problem in the $x - z$ plane.

The transformation formulas between local Cartesian coordinates and oblate spheroidal coordinates are (e.g., [21]):

$$x = c \cosh u \sin\theta \cos\psi \tag{1}$$

$$y = c \cosh u \sin\theta \sin\psi \tag{2}$$

$$z^* = c \sinh u \cos\theta \tag{3}$$

where $0 \le u \le \infty$, $0 \le \theta \le \pi$, $0 \le \psi \le 2\pi$. Moreover, $c$ denotes the semi focal distance given by $c = \sqrt{(a^2 - b^2)}$, while $a$, $b$ correspond to the semi-major and the semi-minor axis of the spheroid, respectively (Figure 1b).

Employing Nicolson notations [22], namely, $\xi = \sinh u$ and $\mu = \cos\theta$, the transformation formulas can be written as:

$$x = c\sqrt{1+\xi^2}\sqrt{1-\mu^2}\cos\psi \tag{4}$$

$$y = c\sqrt{1+\xi^2}\sqrt{1-\mu^2}\sin\psi \tag{5}$$

$$z^* = c\xi\mu \tag{6}$$

## 3. The Boundary Value Problem

The present study deals with the radiation problem of an oblate spheroid, immersed in a liquid field of infinite water depth. The body is assumed to undergo small amplitude oscillations $q_j$, in surge ($j = 1$), sway, ($j = 2$) and heave ($j = 3$). Within the realm of the linear potential theory [23], the resulting velocity and pressure fields can be described in terms of the velocity potential $\Phi(x, y, z, t) = Re\left[\phi(x, y, z)e^{-i\omega t}\right]$, where $t$ is the time, $\omega$ denotes the circular frequency of body's oscillation, $i = \sqrt{-1}$ and $\phi(x, y, z)$ is the spatial complex total radiation potential, which is expressed as:

$$\phi = -i\omega \sum_{j=1}^{3} q_j \phi_j \tag{7}$$

In Equation (7) $\phi_j,\ j = 1, \ldots, 3$, correspond to the unit-amplitude radiation potentials.

The aforementioned potentials $\phi_j$ satisfy, in the entire infinite liquid domain, the Laplace equation given by:

$$\nabla^2 \phi_j = 0 \tag{8}$$

Moreover, the radiation potentials satisfy the following linearized boundary conditions on the free surface (Equation (9)) and on the wetted surface of the submerged body (Equation (10)):

$$K\phi_j + \frac{\partial \phi_j}{\partial z} = 0, \quad z = 0 \tag{9}$$

$$\frac{\partial \phi_j}{\partial n} = n_j \tag{10}$$

where $K = \omega^2/g$, $g$ is the gravitational acceleration and $\mathbf{n} = (n_1, n_2, n_3)$ is the unit vector normal to the boundary of the body.

In the axisymmetric configuration, the surge motions are equivalent to the sway motions, and accordingly only the $j = 1$ and 3 modes are investigated. The unit normals $n_1$ and $n_3$, expressed in oblate spheroidal coordinates, will read:

$$(n_1, n_3) = \left( \frac{\xi_0 \left(1 - \mu^2\right)^{1/2} \cos\psi}{\left(\xi_0^2 + \mu^2\right)^{1/2}}, \quad \frac{\mu \left(\xi_0^2 + 1\right)^{1/2}}{\left(\xi_0^2 + \mu^2\right)^{1/2}} \right) \tag{11}$$

where $\xi_0 = \tanh^{-1}(b/a)$ with $a = c\cosh\xi_0$ and $b = c\sinh\xi_0$.

Except from the above equations, the unit radiation velocity potentials must be zero at infinity away from the free surface (i.e., $\phi_j \to 0,\ z \to \infty$). The overall boundary value problem is completed taking into account the radiation condition for outgoing waves at infinity.

## 4. Formulation of the Radiation Velocity Potentials

The components $\phi_j,\ j = 1$ and 3 of the total radiation potential will be formulated by utilizing the underlying Green's function, connected with the aforementioned boundary value problem. The Green's function (see e.g., [8–12]) can be written as:

$$\begin{aligned} G(x - x', \quad & y - y', \quad z - f) \\ & = \frac{1}{\sqrt{(x-x')^2 + (y-y')^2 + (z-f)^2}} \\ & - \frac{1}{2\pi} \int_0^{\infty} \int_{-\pi}^{\pi} \frac{K+k}{K-k} e^{-k(z+f)} e^{ik[(x-x')cosa + (y-y')sina]} dadk \end{aligned} \tag{12}$$

where $(x, y, z-f)$ are the coordinates of the source point and $(x', y', 0)$ are the coordinates of the field point.

Clearly, Equation (12) satisfies the Laplace equation (Equation (8)), the free-surface condition (Equation (9)) and the far-field condition as $z \to \infty$. Nevertheless, the Green's function does not satisfy the radiation condition for outgoing waves at infinity. This task is accomplished by interpreting the infinite improper integral as a Cauchy principal value integral, namely, by introducing in Equation (12) the following notations [16]:

$$\int_0^\infty \frac{F(k)}{K-k}dk = PV\int_0^\infty \frac{F(k)}{K-k}dk - i\pi F(K) \tag{13}$$

where $PV$ denotes the Cauchy principal value integral.

The Green's function (Equation (12)) must be properly elaborated in order to be expanded in multipoles. The multipoles [4] of the Green's function are obtained by employing the image singularity system for an oblate spheroid. The aforementioned theorem for the axisymmetric configuration of an oblate spheroid is expressed by the following formula [16]:

$$P_n^m(\mu)Q_n^m(i\xi)cosm\psi = \frac{(-1)^m}{2\pi P_n^m(i0)}\frac{(n+m)!}{(n-m)!}\int_0^{2\pi}\int_0^1 \frac{P_n^m(\mu')cosm\psi'}{(x-x')^2+(y-y')^2+z^2}d\mu' d\psi' \tag{14}$$

where $P_n^m$ and $Q_n^m$ are the $n$th degree and $m$th order associate Legendre functions, of the first and the second kind, respectively. In the succeeding discussion, the orientation of the local vertical $z^*$ axis (Figure 1b) will be reversed, and it will be associated with the global $z$ axis with the relationship $z = f - z^*$.

Substituting Equation (14) into Equation (12), the multipoles of the Green's function (auxiliary potentials), coined herein $G_n^m$, take the form:

$$\begin{aligned} &G_n^m(x-x', y-y', z) \\ &= P_n^m(\mu)Q_n^m(i\xi)cosm\psi - \tfrac{1}{(2\pi)^2}\tfrac{(-1)^m}{P_n^m(i0)}\tfrac{(n+m)!}{(n-m)!} \\ &\times\int_0^\infty\int_{-\pi}^{\pi}\int_0^{2\pi}\int_0^1 \tfrac{K+k}{K-k}e^{-k(z+f)}e^{ik[(x-x')cosa+(y-y')sina]}P_n^m(\mu')cosm\psi' dadkd\mu' d\psi' \end{aligned} \tag{15}$$

It is evident that Equation (15) must be elaborated further, in order to express the second term of the equation into oblate spheroidal coordinates. This is achieved by employing the following expansion of the exponential term into spheroidal coordinates [16]:

$$e^{kz^*+ik(xcosa+ysina)} = \sum_{s=0}^\infty\sum_{t=0}^s \left(A_s^t\cos t\psi + B_s^t\sin t\psi\right)P_s^t(\mu)P_s^t(i\xi_0) \tag{16}$$

where

$$\begin{pmatrix} A_s^t \\ B_s^t \end{pmatrix} = (-1)^s i^{s-t}\varepsilon_t\frac{(s-t)!}{(s+t)!}(2s+1)\sqrt{\frac{\pi}{2kc}}J_{s+1/2}(kc)\begin{pmatrix} costa \\ sinta \end{pmatrix} \tag{17}$$

and $J_\lambda$ denotes the Bessel function of the first kind with fractional order $\lambda$.

Therefore, the final expression for the auxiliary multipole expansions of the Green's function for the oblate spheroid reads:

$$G_n^m(i\xi,\mu,\psi) = P_n^m(\mu)Q_n^m(i\xi)\cos m\psi + \sum_{s=0}^\infty\sum_{t=0}^s C_{ns}^{mt}P_n^m(\mu)P_n^m(i\xi)\cos t\psi \tag{18}$$

with

$$\begin{aligned} C_{ns}^{mt} &= -\tfrac{1}{4c}(-1)^{n+s} i^{n+s-m-t} \tfrac{2\pi}{\varepsilon_m} \varepsilon_t \tfrac{(n+m)!}{(n-m)!} \tfrac{(s-t)!}{(s+t)!} (2s+1) \\ &\times \delta_{tm} \Big( PV \int_0^\infty \tfrac{K+k}{K-\kappa} e^{-2kf} \tfrac{1}{k} J_{n+1/2}(kc) J_{s+1/2}(kc) dk \\ &-2\pi i e^{-2Kf} J_{n+1/2}(Kc) J_{s+1/2}(Kc) \Big) \end{aligned} \tag{19}$$

In Equation (19), $\varepsilon_m$ is the Newman symbol ($\varepsilon_0 = 2$, $\varepsilon_m = 1$ for $= 1, 2, 3, \ldots$), $\delta_{tm}$ is the Kronecker's delta function, and $PV$ denotes the Cauchy principal value integral.

Having defined the auxiliary multipole expansions of the Green's function, $G_n^m$, the $j$th velocity potential is immediately obtained from:

$$\phi_j = \sum_{n=0}^{\infty} \sum_{m=0}^{n} F_n^m G_n^m \tag{20}$$

where $F_n^m$ are unknown coefficients to be obtained by employing the body boundary condition.

The final form for each velocity potential $j = 1$ and 3 will read:

$$\phi_j = \sum_{n=0}^{\infty} \sum_{m=0}^{n} F_n^m P_n^m(\mu) Q_n^m(i\xi) \cos m\psi + \sum_{n=0}^{\infty} \sum_{m=0}^{n} F_n^m \sum_{s=0}^{\infty} \sum_{t=0}^{s} C_{ns}^{mt} P_s^t(\mu) P_s^t(i\xi) \cos t\psi \tag{21}$$

The velocity potentials are fully determined by calculating the coefficients $F_n^m$. To achieve this goal, the body boundary condition (Equation (10)) is applied for each mode of oscillation, using Equation (21) as the expression for the velocity potential. The body conditions for the radiation problem read:

$$\left. \frac{\partial \phi_1}{\partial \xi} \right|_{\xi=\xi_0} = n_1 = -bP_1^1(\mu) \cos\psi \tag{22}$$

$$\left. \frac{\partial \phi_3}{\partial \xi} \right|_{\xi=\xi_0} = n_3 = aP_1^0(\mu) \tag{23}$$

Taking into account Equations (22) and (23), and making use of the orthogonality properties of the trigonometric and the associated Legendre functions (see e.g., [16]), the following linear system of equations are obtained to be solved, using standard matrix techniques, in terms of the expansion coefficients $F_n^m$:

$$F_l^r + \sum_{n=0}^{\infty} \sum_{m=0}^{n} a_l^r F_n^m C_{nl}^{mr} = i \frac{b}{a} \frac{\delta_{1r}\delta_{1l}}{\dot{Q}_l^r(i\xi_0)} \tag{24}$$

$$F_l^r + \sum_{n=0}^{\infty} \sum_{m=0}^{n} a_l^r F_n^m C_{nl}^{mr} = -i \frac{\delta_{or}\delta_{1l}}{\dot{Q}_l^r(i\xi_0)} \tag{25}$$

where $a_l^r = \dot{P}_l^r(i\xi_0)/\dot{Q}_l^r(i\xi_0)$ and the upper dot denotes differentiation with respect to the argument.

## 5. Hydrodynamic Coefficients in Surge and Heave

Having calculated the radiation potentials, the sought hydrodynamic parameters are obtained via the surface integral:

$$\mu_{ij} - \frac{i}{\omega} \lambda_{ij} = -\rho \int_{S_0} \phi_i n_j dS \tag{26}$$

where $\mu_{ij}$ and $\lambda_{ij}, i, j = 1$ and 3 denote the added mass and hydrodynamic damping coefficients, respectively, while $\rho$ is the water density. The integration is performed on the wetted surface $S_0$ of the spheroid.

The differential area, $dS$, in spheroidal coordinates for an oblate spheroid is written as:

$$dS = a\left(\xi_0^2 + \mu^2\right)^{1/2} d\mu d\psi \tag{27}$$

Substituting the radiation potentials (Equation (21)) and the unit normals (Equation (11)) into Equation (26), one gets, after evaluating the surface integral over $S_0$, the following:

$$\mu_{11} - \frac{i}{\omega}\lambda_{11} = \frac{1}{a\dot{P}_1^1(i\xi_0)}\left(\frac{i\,b\,P_1^1(i\xi_0)}{a} + \frac{2F_1^1}{\xi_0^2+1}\right) \tag{28}$$

$$\mu_{33} - \frac{i}{\omega}\lambda_{33} = \frac{1}{b\dot{P}_1^0(i\xi_0)}\left(i\,P_1^0(i\xi_0) + \frac{F_1^0}{\xi_0^2+1}\right) \tag{29}$$

It is recalled that for the axisymmetric case of the spheroid, $\mu_{11} = \mu_{22}$ and $\lambda_{11} = \lambda_{22}$. Clearly, the off-diagonal terms $\mu_{31}$, $\mu_{13}$, $\lambda_{31}$, $\lambda_{13}$ are zero. In the following section, the added mass and hydrodynamic damping coefficients are normalized by $4/3\pi\rho ba^2$ and $4/3\pi\rho ba^2\omega$ respectively, unless otherwise mentioned.

## 6. Results and Discussion

For demonstrating the accuracy of the developed semi-analytical formulation, results of the present method are compared against the results of Wu [18] for the limiting case of a sphere, and against calculations obtained using the code WAMIT [19], which is based on the well-known Boundary Integral Equation Method (BIEM). In the case of Wu [18], who studied the diffraction and the radiation problem of a single and a group of immersed spheres, the oblate spheroid is simulated as a sphere assuming $a \to b$, and comparisons are made for an immersion depth $f$ equal to $1.5a$. The corresponding results are shown in Figure 2, where the added mass and the damping coefficients are normalized by $4/3\pi\rho a^3$ and $4/3\pi\rho a^3\omega$ respectively. The abbreviation ISS, which stands for Image Singularity System, is used to denote the present analytical formulation. In the case of WAMIT [19], comparisons are made for an oblate spheroid of slenderness $a/b = 1.25$, and for two immersion depths, $f$, equal to $1.01a$ and $1.5a$. The immersion of $f = 1.01a$ has been selected so that the body touches the free surface. The relevant results are shown in Figures 3 and 4. From Figures 2–4, it is immediately apparent that the results of the present method demonstrate an excellent agreement with both the results of Wu [18] for the limiting case of the sphere (average relative error smaller than 0.1%), as well as with the results obtained using WAMIT [19].

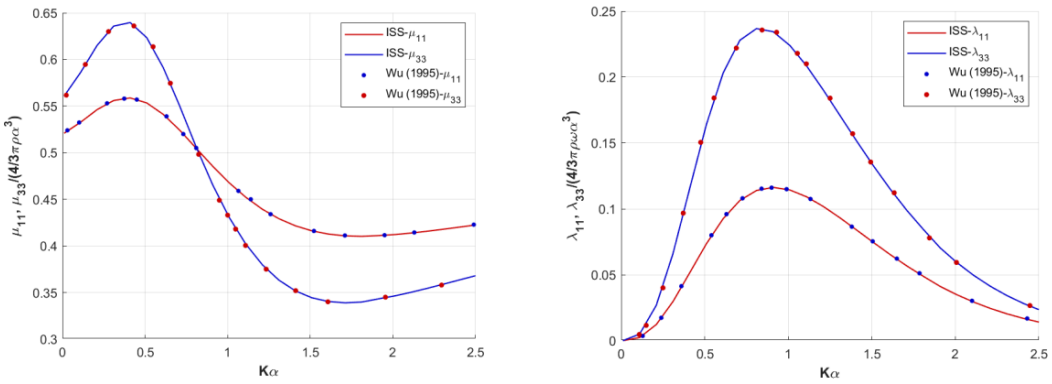


(**a**) (**b**)

**Figure 2.** Normalized hydrodynamic coefficients for a sphere ($a \to b$ in the case of ISS) immersed at $f = 1.5a$: (**a**) Surge and heave added mass; (**b**) Surge and heave hydrodynamic damping.

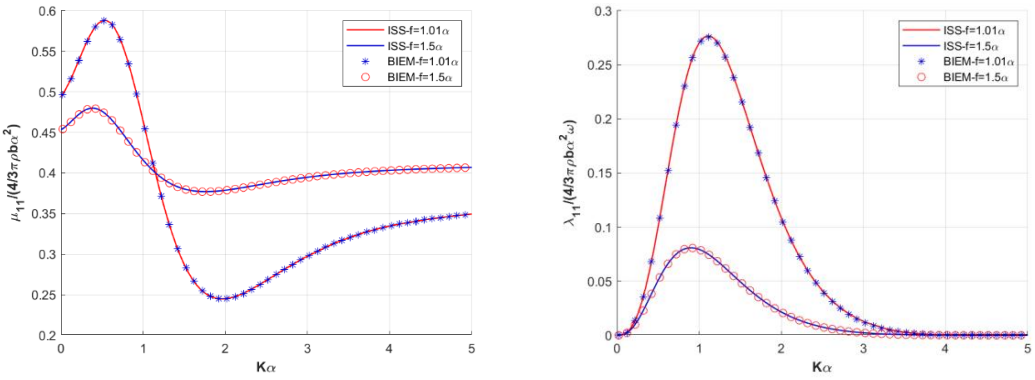


**Figure 3.** Normalized hydrodynamic coefficients in surge for $a/b = 1.25$: (**a**) Surge added mass; (**b**) Surge hydrodynamic damping.

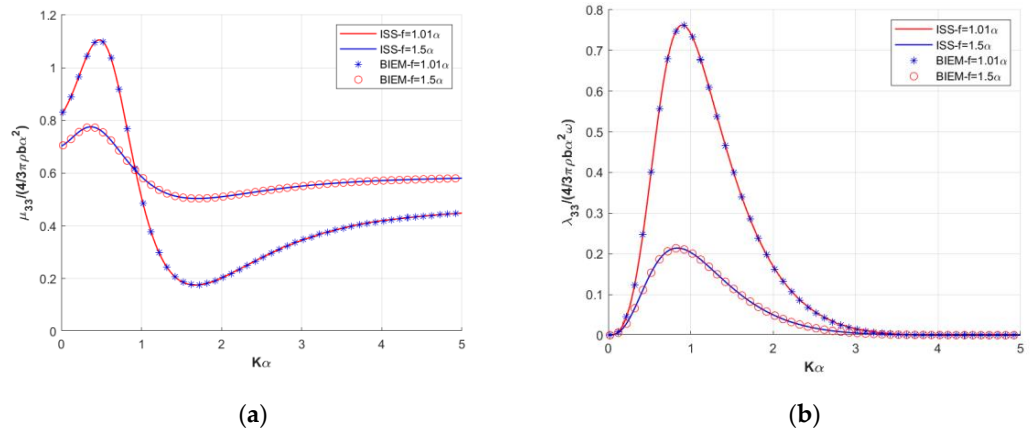


**Figure 4.** Normalized hydrodynamic coefficients in heave for $a/b = 1.25$: (**a**) Heave added mass; (**b**) Heave hydrodynamic damping.

The numerical computations of Figures 2–4 have been realized by utilizing $n = 5$ modes (in the semi-analytical formulation), which was proven sufficient to achieve a convergence up to the fifth decimal digit (Tables 1 and 2).

**Table 1.** Convergence sequence of the normalized surge added mass and damping coefficients for several mode numbers (Oblate spheroid with $a/b = 1.25$ and immersion $f = 1.5a$ ).

| $Ka$ | $n = 2$ | | $n = 5$ | | $n = 8$ | |
|---|---|---|---|---|---|---|
| | $\mu_{11}$ | $\lambda_{11}$ | $\mu_{11}$ | $\lambda_{11}$ | $\mu_{11}$ | $\lambda_{11}$ |
| 0.1 | 0.45812 | 0.00043 | 0.45814 | 0.00043 | 0.45814 | 0.00043 |
| 0.2 | 0.47086 | 0.00797 | 0.47090 | 0.00797 | 0.47090 | 0.00797 |
| 0.3 | 0.47923 | 0.02498 | 0.47929 | 0.02499 | 0.47929 | 0.02499 |
| 0.4 | 0.47986 | 0.03533 | 0.47994 | 0.03535 | 0.47994 | 0.03535 |
| 0.5 | 0.47356 | 0.05548 | 0.47367 | 0.05555 | 0.47367 | 0.05555 |
| 0.6 | 0.46727 | 0.06394 | 0.46739 | 0.06405 | 0.46739 | 0.06405 |
| 0.7 | 0.45089 | 0.07578 | 0.45099 | 0.07599 | 0.45099 | 0.07599 |
| 0.8 | 0.44182 | 0.07898 | 0.44190 | 0.07924 | 0.44190 | 0.07924 |
| 1.0 | 0.41590 | 0.07908 | 0.41579 | 0.07943 | 0.41579 | 0.07943 |
| 2.0 | 0.37901 | 0.02195 | 0.37876 | 0.02154 | 0.37876 | 0.02154 |
| 3.0 | 0.39457 | 0.00249 | 0.39477 | 0.00231 | 0.39477 | 0.00231 |
| 4.0 | 0.40317 | 0.00016 | 0.40330 | 0.00014 | 0.40330 | 0.00014 |
| 5.0 | 0.40691 | 0.00001 | 0.40698 | 0.00001 | 0.40698 | 0.00001 |

**Table 2.** Convergence sequence of the normalized heave added mass and damping coefficients for several mode numbers (Oblate spheroid with $a/b = 1.25$ and immersion $f = 1.5a$ ).

| $Ka$ | $n = 2$ | | $n = 5$ | | $n = 8$ | |
|---|---|---|---|---|---|---|
| | $\mu_{33}$ | $\lambda_{33}$ | $\mu_{33}$ | $\lambda_{33}$ | $\mu_{33}$ | $\lambda_{33}$ |
| 0.1 | 0.72471 | 0.00371 | 0.7248 | 0.00371 | 0.7248 | 0.00371 |
| 0.2 | 0.75182 | 0.02264 | 0.75196 | 0.02265 | 0.75196 | 0.02265 |
| 0.3 | 0.77128 | 0.05792 | 0.77148 | 0.05795 | 0.77148 | 0.05795 |
| 0.4 | 0.77458 | 0.10229 | 0.77487 | 0.10239 | 0.77487 | 0.10239 |
| 0.5 | 0.75989 | 0.14589 | 0.76026 | 0.14613 | 0.76026 | 0.14613 |
| 0.6 | 0.73095 | 0.18078 | 0.73134 | 0.18123 | 0.73134 | 0.18123 |
| 0.7 | 0.69406 | 0.20307 | 0.69437 | 0.20377 | 0.69437 | 0.20377 |
| 0.8 | 0.65526 | 0.2126 | 0.65537 | 0.21352 | 0.65537 | 0.21352 |
| 0.9 | 0.61886 | 0.21142 | 0.61866 | 0.21249 | 0.61866 | 0.21249 |
| 1.0 | 0.58728 | 0.2024 | 0.58673 | 0.20349 | 0.58673 | 0.20349 |
| 2.0 | 0.51126 | 0.05129 | 0.51061 | 0.05002 | 0.51061 | 0.05002 |
| 3.0 | 0.55043 | 0.00593 | 0.55104 | 0.0054 | 0.55103 | 0.00539 |
| 4.0 | 0.57154 | 0.0004 | 0.57194 | 0.00033 | 0.57194 | 0.00033 |
| 5.0 | 0.58083 | 0.00002 | 0.58107 | 0.00001 | 0.58107 | 0.00001 |

Figures 5 and 6 show the effect of the immersion depth on the surge and heave hydrodynamic coefficients respectively, for an oblate spheroid with slenderness ratio $a/b = 1.1$. More specifically, three different immersion depths, $f$, are examined equal to $1.01a$, $1.5a$ and $2a$. It can be easily observed that the increase of $f$ leads to a smoother variation of the surge (Figure 5a) and the heave (Figure 6a) added mass in the examined $Ka$ interval. As expected, by increasing the distance between the spheroid and the undisturbed free surface, the surge and the heave hydrodynamic damping coefficients (Figures 5b and 6b, respectively) decrease. In general, as $f$ increases, both added mass and damping tend to become frequency-independent hydrodynamic quantities. Analogous conclusions can be drawn for $a/b = 1.25$ (Figures 3 and 4). It is also interesting to note that, for a given immersion depth, the increase of the slenderness of the spheroid decreases the damping coefficients, while the added mass exhibits a reversed behavior. This can be demonstrated by comparing the curves of $f = 1.01a$ and $f = 1.5a$, in Figures 3 and 4 ($a/b = 1.25$), with the corresponding ones of Figures 5 and 6 ($a/b = 1.1$).

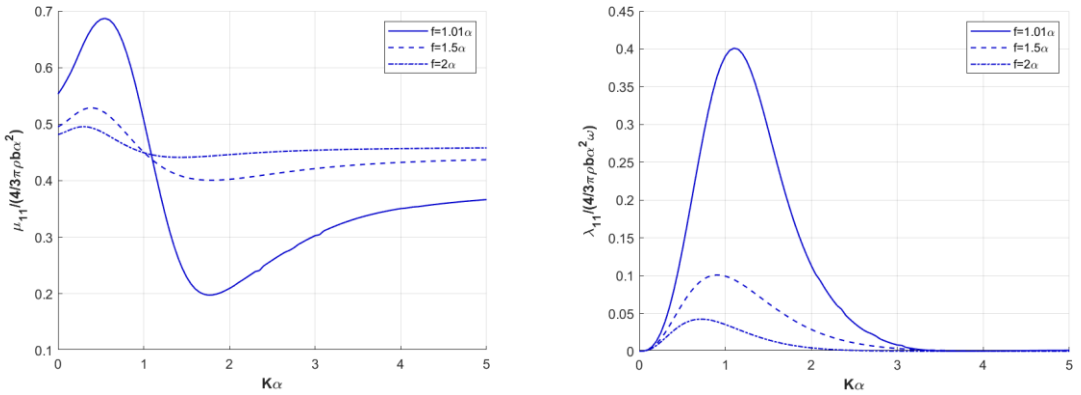


(**a**) (**b**)

**Figure 5.** Effect of immersion, $f$, on the normalized surge hydrodynamic coefficients for an oblate spheroid of $a/b = 1.1$: (**a**) Surge added mass; (**b**) Surge hydrodynamic damping.

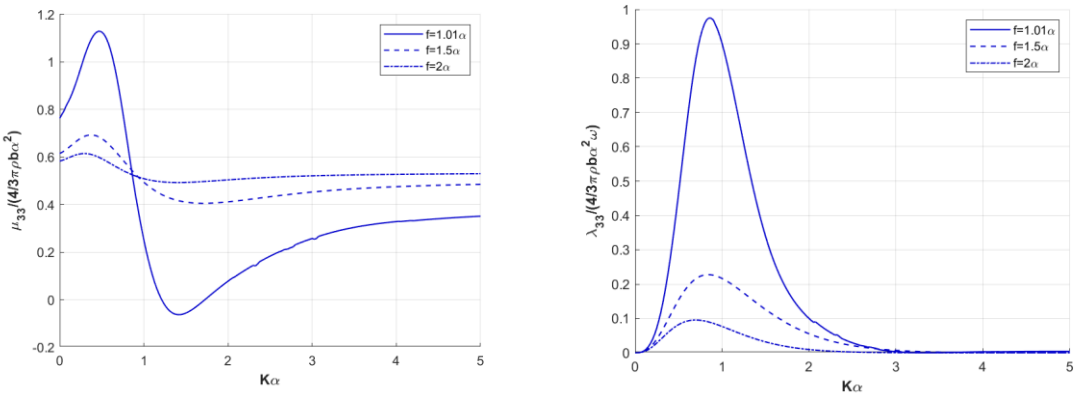


(**a**) (**b**)

**Figure 6.** Effect of immersion, $f$, on the normalized heave hydrodynamic coefficients for an oblate spheroid of $a/b = 1.1$: (**a**) Heave added mass; (**b**) Heave hydrodynamic damping.

## 7. Conclusions

In the present paper, a semi-analytical formulation has been developed for solving the radiation problem of a fully submerged oblate spheroid in a liquid field of infinite depth. The placement of the examined body is "axisymmetric"; namely, the symmetrical axis is normal to the free surface. The radiation problem is solved for all translational degrees of freedom, and formulas for calculating the corresponding hydrodynamic coefficients are derived. The employed method is based on the expansion of the governing Green's function into spheroidal harmonics, using the method of ultimate image singularities. The excellent agreement of results with those of Wu [18] for the limiting case of a sphere, and with those obtained using a well-known BIEM code, demonstrates the accuracy, reliability, and robustness of the developed semi-analytical solution.

Moreover, the results of the present paper illustrated that the immersion depth and the slenderness of the oblate spheroid have a direct impact on the hydrodynamic coefficients. Specifically, for a given slenderness, the placement of the spheroid at a greater distance from the free surface leads to a more smooth variation of the added mass coefficients, as well as to a reduction of the damping coefficients. The increase of the slenderness of the spheroid for a given immersion depth affects the hydrodynamic coefficients in a similar manner, i.e., the damping coefficient decreases, and the added mass exhibits a decrease of the absolute difference between the observed maximum and minimum values.

The present numerical formulation, combined with the corresponding solution of the diffraction problem [17], could be further exploited for calculating the translational motions of submerged spheroids, with potential application to wave energy hydrodynamic problems, i.e., numerical modelling of submerged point absorbers.

**Author Contributions:** Conceptualization, I.K.C.; methodology, I.K.C. and E.I.A.; software, I.K.C., E.I.A. and E.L.; validation, E.I.A. and E.L.; investigation, I.K.C., E.I.A. and E.L.; writing—original draft preparation, E.I.A.; writing—review and editing, E.L. and I.K.C. All authors have read and agreed to the published version of the manuscript.

**Funding:** This research was co-financed by Greece and the European Union (European Social Fund-ESF) through the Operational Programme "Human Resources Development, Education and Lifelong Learning" in the context of the project "Strengthening Human Resources Research Potential via Doctorate Research" (MIS-5000432), implemented by the State Scholarships Foundation (IKϒ).

**Conflicts of Interest:** The authors declare no conflict of interest.

## References


1. Linton, C.M. Radiation and diffraction of water waves by a submerged sphere in finite depth. *Ocean Eng.* **1991**, *18*, 61–74. [CrossRef]
2. Wu, G.X.; Witz, J.A.; Ma, Q.; Brown, D.T. Analysis of wave induced drift forces acting on a submerged sphere in finite water depth. *Appl. Ocean Res.* **1994**, *16*, 353–361. [CrossRef]
3. Rahman, M. Simulation of diffraction of ocean waves by submerged sphere in finite depth. *Appl. Ocean Res.* **2001**, *23*, 305–317. [CrossRef]
4. Thorne, R.C. Multipole expansions in the theory of surface waves. *Math. Proc. Camb.* **1953**, *49*, 707–716. [CrossRef]
5. Havelock, T.H. The moment on a submerged solid of revolution moving horizontally. *Q. J. Mech. Appl. Math.* **1952**, *5*, 129–136. [CrossRef]
6. Havelock, T.H. The forces on a submerged body moving under waves. *Trans. Inst. Nav. Arch.* **1954**, *96*, 77–88.
7. Miloh, T. The ultimate image singularities for external ellipsoidal harmonics. *SIAM J. Appl. Math.* **1974**, *26*, 334–344. [CrossRef]
8. Chatjigeorgiou, I.K.; Miloh, T. Wave scattering of spheroidal bodies below a free surface. *J. Ship Res.* **2013**, *57*, 141–154. [CrossRef]
9. Chatjigeorgiou, I.K.; Miloh, T. Free-surface hydrodynamics of a submerged prolate spheroid in infinite water depth based on the method of multipole expansions. *Q. J. Mech. Appl. Math.* **2014**, *67*, 525–552. [CrossRef]
10. Chatjigeorgiou, I.K.; Miloh, T. Hydrodynamics of submerged prolate spheroids advancing under waves: Wave diffraction with forward speed. *J. Fluids Struct.* **2014**, *49*, 202–222. [CrossRef]
11. Chatjigeorgiou, I.K.; Miloh, T. Hydrodynamic wave resistance and diffraction problems of submerged prolate spheroids based on a Green's function image singularities method. *Eur. J. Mech. B Fluids* **2015**, *49*, 184–1966. [CrossRef]
12. Chatjigeorgiou, I.K.; Miloh, T. Radiation and oblique diffraction by submerged prolate spheroids in water of finite depth. *J. Ocean Eng. Mar. Energy* **2015**, *1*, 3–18. [CrossRef]
13. Wu, G.X.; Taylor, R.E. The exciting force on a submerged spheroid in regular waves. *J. Fluid Mech.* **1987**, *182*, 411–426. [CrossRef]
14. Wu, G.X.; Taylor, R.E. On radiation and diffraction of surface waves by submerged spheroids. *J. Ship Res.* **1989**, *33*, 84–92.
15. Chatjigeorgiou, I.K. The analytic solution for hydrodynamic diffraction by submerged prolate spheroids in infinite water depth. *J. Eng. Math.* **2013**, *81*, 47–65. [CrossRef]
16. Chatjigeorgiou, I.K. *Analytical Methods in Marine Hydrodynamics*; Cambridge University Press: Cambridge, UK, 2018.
17. Chatjigeorgiou, I.K.; Loukogeorgaki, E.; Anastasiou, E.; Mantadakis, N. Ultimate image singularities in oblate spheroidal coordinates with applications in hydrodynamics. *J. Mar. Sci. Eng.* **2020**, *8*, 32. [CrossRef]
18. Wu, G.X. The interactions of water waves with a group of submerged spheres. *Appl. Ocean Res.* **1995**, *17*, 165–184. [CrossRef]
19. WAMIT. *User Manual for WAMIT Versions 6.3*; 6.3PC, 6.3S, 6.3S-PC; WAMIT: Chestnut Hill, MA, USA, 2006.
20. Loukogeorgaki, E.; Boufidi, I.; Chatjigeorgiou, I.K. Performance of an array of oblate spheroidal heaving wave energy converters in front of a wall. *Water* **2020**, *12*, 188. [CrossRef]
21. Moon, P.H.; Spencer, D.E. *Field Theory Handbook: Including Coordinate Systems, Differential Equations, and Their Solutions*, 2nd ed.; Spinger: Berlin, Germany, 1988.
22. Nicholson, J.W. Oblate spheroidal harmonics and their applications. *Philos. T. R. Soc. A* **1924**, *224*, 49–93. [CrossRef]
23. Newman, J.N. *Marine Hydrodynamics*; MIT Press: Cambridge, MA, USA, 1977.